Preprints of the 19th World Congress
The International Federation of Automatic Control
Cape Town, South Africa. August 24-29, 2014

Finding the Optimal Aeration Profiles and DO Profiles in a Plug-flow Biological Wastewater Treatment Reactor with A Theoretical Approach

Xiaoxin. Liu*'. Yuanwei. Jing*. Gustaf Olsson ***. Zhiguo. Yuan****

*College of Information Science and Engineering, Northeastern University, Shenyang, Liaoning, 110004. P.R.China. (e-mail:liuxiaoxin0408@163.com, ywjjing@mail.neu.edu.cn).
**Advanced Water Management Centre, The University of Queensland, St. Lucia, Brisbane, QLD, 4072, Australia. (e-mail: z.yuan@awmc.uq.edu.au).
*** Lund University, Lund, 22100, Sweden. (gustaf.olsson@iea.lth.se)

Abstract: It is a common principle that aeration to a wastewater treatment reactor performing aerobic carbon and ammonium oxidation should be minimised while satisfactory carbon and ammonium removal is achieved. The implementation of this principle in a plug-flow like aerobic reactor has so far been in an ad-hoc manner in the absence of a theoretically optimal dissolved oxygen (DO) profile. In this study, the Pontryagin Maximum Principle is applied to derive the theoretically optimal DO profile along a plug-flow aerobic reactor. While it is difficult to implement this optimisation algorithm online in practice due to the requirement of detailed wastewater composition and model parameter information, the optimal aeration profiles revealed under various conditions provide guidance to the design and operation of aeration systems. The optimal K_La and DO profiles can be applied in benchmark model to not only achieve satisfactory effluent requirements but also aeration energy is saved.

Keywords: Aeration, Biological wastewater treatment, Control, Maximum Principle, Optimal, Plug-flow, Simulation benchmark, Two-point boundary-value problem.

1. INTRODUCTION

Aeration in a wastewater treatment plant is an energy intensive process, transferring oxygen in gas phase to dissolved oxygen (DO). The DO concentration is also crucial for the biological process to operate satisfactorily. Control of aeration systems becomes even more important when treatment plants face more stringent discharge limits and when energy efficiency is high up on the agenda. This motivates appropriate aeration control. An overview of aeration control during the last decade is found in Åmand et al. (2013).

In a plug flow reactor, the biological activity is the largest at the inlet area of the aerator. Consequently the air flow demand is high in this area. As the biological reactions goes to completion towards the outlet area the air flow requirement will decrease to small levels. This fact was realized very early (Olsson, 2012). However, it was difficult to implement an air flow distribution along the aerator that would satisfy this requirement. Instead, a uniform air flow was most often implemented. This resulted in low DO concentrations in the inlet area and too high DO concentrations towards the outlet.

It is intuitively obvious that the desired air flow supply along the reactor should be the "inverse" of the DO profile with a uniform air flow. In other words, the air supply should be high in the inlet area and gradually decrease towards a low value towards the outlet of the aerator.

The aeration could be controlled individually and this resulted in a DO concentration that could be kept closer to a desired setpoint along the aerator. Naturally, such a system is more complex and requires the remote control of several air flow valves as well as an air supply system with a compressor (blower) that can deliver a variable air flow rate, often in a wide operating range. Blowers supplied with variable frequency drives (VFD) allow a flexible control of the aeration capacity.

As a distributed parameter system, a plug-flow like aerobic reactor offers more flexibility for aeration control, namely different DO set-points can be selected for different zones in the reactor provided that the aeration facilities in these zones can be operated independently. However, it also dramatically increases the complexity of the control problem. In this case the ammonia concentration towards the outlet will determine the DO setpoints (Åmand et al., 2012). There is currently no consensus how aeration in a plug-flow like nitrifying reactor should be controlled.

The Pontryagin Maximum Principle (Bryson and Ho, 1975) and an optimisation algorithm have been applied to derive the theoretically optimal air supply distribution and DO profile along a plug-flow aerobic reactor. The air supply is here represented by the oxygen transfer rate K_La. Although it is too complex to apply the optimisation algorithm online in a full-scale plant due to the demand of detailed wastewater composition and related model parameter information, the optimal K_La and DO profiles can provide guidance to the

design and operation of aeration systems under different operating conditions.

2. PROBLEM FORMULATION

2.1 *Plant description*

The case study is designed based on the IWA benchmark model (Copp, 1999). The plug-flow aerobic reactor has a volume of 4000 m3, the total volume of the three aerobic reactors in the benchmark model, and a length of 50 m. The average and the dynamic dry weather flow (flowrate and wastewater composition), as specified in Copp (1999), were used in the steady state and dynamic simulation studies, respectively.

2.2 *Model*

Many models have been proposed for the aerobic processes in activated sludge systems. The IWA Activated Sludge Models (ASM) No. 1, 2 and 3 (Henze et al., 2000) provide a good summary of these models. The following simpler yet realistic model is tailored from ASM1 and ASM3 and used for the design of optimal aeration control (the self-explanatory symbols can be found in ASM1&3(Henze et al., 2000)).

$$\begin{aligned}
\frac{\partial S_{NH}(z,t)}{\partial t} &= -\frac{Q(t)}{A}\frac{\partial S_{NH}(z,t)}{\partial z} - \frac{\mu_A(z,t)}{Y_A} - i_{NBM}\mu_H(z,t) + \frac{i_{NSS}}{Y_H}\mu_H(z,t) \\
&\quad + (i_{NXS} - Y_H i_{NBM}) r_h(z,t) + i_{NBM}(1-f_P)(b_A X_A + b_H X_H) \\
\frac{\partial S_{COD}(z,t)}{\partial t} &= -\frac{Q(t)}{A}\frac{\partial S_{COD}(z,t)}{\partial z} - \frac{\mu_H(z,t)}{Y_H} \\
\frac{\partial S_O(z,t)}{\partial t} &= -\frac{Q(t)}{A}\frac{\partial S_O(z,t)}{\partial z} - \frac{4.57 - Y_A}{Y_A}\mu_A(z,t) - \frac{1-Y_H}{Y_H}\mu_H(z,t) \\
&\quad - (1-Y_H) r_h(z,t) - (1-f_P)(b_A X_A + b_H X_H) + K_L a(z,t)\left(S_O^* - S_O(z,t)\right) \\
\frac{\partial X_S(z,t)}{\partial t} &= -\frac{Q(t)}{A}\frac{\partial X_S(z,t)}{\partial z} - r_h(z,t)
\end{aligned} \tag{1}$$

with boundary conditions

$$S_{NH}(0,t), S_{COD}(0,t), S_O(0,t), X_S(0,t),$$
$$S_{NH}(z,0), S_{COD}(z,0), S_O(z,0) \text{ and } X_S(z,0)$$

and reaction kinetics

$$\begin{aligned}
\mu_A(z,t) &= \mu_{A,\max}\frac{S_{NH}(z,t)}{S_{NH}(z,t)+K_{NH}}\frac{S_O(z,t)}{S_O(z,t)+K_{OA}}X_A \\
\mu_H(z,t) &= \mu_{H,\max}\frac{S_{COD}(z,t)}{S_{COD}(z,t)+K_S}\frac{S_O(z,t)}{S_O(z,t)+K_{OH}}X_H \\
r_h(z,t) &= k_H\frac{X_S(z,t)/X_H}{K_X + X_S(z,t)/X_H}X_H
\end{aligned} \tag{2}$$

2.3 *Objective function*

The objective is to control aeration to the reactor (i.e. determining $K_L a(z,t)$) such that the aeration energy consumption is minimised while the effluent ammonium and COD discharge limits are met. In this paper, the following formula is employed to calculate the aeration energy consumption, according to Copp (1999):

$$J = \frac{1}{T}\int_0^T \int_0^l \left[k_1 K_L a(z,t)^2 + k_2 K_L a(z,t)\right] A dz dt, \tag{3}$$

Where k_1=0.0073, k_2=0.1412, T is the optimisation horizon, l is the length of the reactor.

2.4 *Constraints*

$$\begin{aligned}
&K_L a_{\min} \le K_L a(z,t) \le K_L a_{\max} && (C1) \\
&S_{NH}(l,t) \le S_{NH.\lim} && (C2) \\
&S_{COD}(l,t) \le S_{COD.\lim} \quad \forall t \in [0,T], \forall z \in [0,l] && (C3) \\
&S_{NH}(z,t) \ge 0 && (C4) \\
&S_{COD}(z,t) \ge 0 && (C5) \\
&S_O(z,t) \ge 0 && (C6)
\end{aligned} \tag{4}$$

3. FINDING THE OPTIMAL AERATION PROFILES AND DO PROFILES

The optimal control problem defined by Model(1), Objective function(3) and Constraints(4) above is solved in two steps, using the Pontryagin Maximum Principle (see e.g. Bryson and Ho, 1975). The optimal control is first found for a steady state reactor; the results are then applied to a dynamically loaded reactor.

3.1 *Optimal control for a steadily loaded reactor*

In steady state, the derivatives on the left hand sides of model equations (1) become zero, resulting in the following steady-state equations:

$$\begin{aligned}
\frac{\partial S_{NH}(z)}{\partial z} &= -\frac{A}{Q}\frac{\mu_A(z)}{Y_A} - \frac{A}{Q}i_{NBM}\mu_H(z) + \frac{A}{Q}\frac{i_{NSS}}{Y_H}\mu_H(z) + \frac{A}{Q}(i_{NXS} - Y_H i_{NBM}) r_h(z) \\
&\quad + \frac{A}{Q}i_{NBM}(1-f_P)(b_A X_A + b_H X_H) \\
\frac{\partial S_{COD}(z)}{\partial z} &= -\frac{A}{Q}\frac{\mu_H(z)}{Y_H} \\
\frac{\partial S_O(z)}{\partial z} &= -\frac{A}{Q}\frac{4.57 - Y_A}{Y_A}\mu_A(z) - \frac{A}{Q}\frac{1-Y_H}{Y_H}\mu_H(z) - \frac{A}{Q}(1-Y_H) r_h(z) \\
&\quad - \frac{A}{Q}(1-f_P)(b_A X_A + b_H X_H) + \frac{A}{Q}K_L a(z)\left(S_O^* - S_O(z)\right) \\
\frac{\partial X_S(z)}{\partial z} &= -\frac{A}{Q} r_h(z)
\end{aligned} \tag{5}$$

with boundary conditions simplified to $S_{NH}(0)$, $S_{COD}(0)$,$S_O(0)$ and $X_S(0)$. The reaction kinetics $\mu_A(z)$, $\mu_H(z)$ and $\gamma_h(z)$ are defined by the equation (2) but with the independent variable t eliminated. The objective function is simplified to:

$$J = \int_0^l \left[k_1 K_L a(z)^2 + k_2 K_L a(z)\right] A dz \tag{6}$$

The control and state constraints are defined in (4) with the independent variable t eliminated.

For notional purpose, we define a state vector $x(z)=[S_{NH}(z)\ S_{COD}(z)\ S_O(z)\ X_S(z)]^T$, a function vector $f(z)=[f_1\ f_2\ f_3\ f_4]^T$,

Where f_i (i=1,2,3,4) is the right hand side function of the i-th state equation in (5), and a scalar function:

$$L(z)=k_1K_La(z)^2+k_2K_La(z)$$

The optimisation problem is simplified to find an optimal profile of K_La along the reactor such that J as defined in (6) is minimised subject to the constraints. Solving the optimisation problem defined above requires defining the *Hamiltonian function* (Bryson and Ho, 1975) as follows:

$$H=L(z)+\boldsymbol{\lambda}^T(z)\mathbf{f}(z)$$

Where $\boldsymbol{\lambda}(z)=[\lambda_1(z)\ \lambda_2(z)\ \lambda_3(z)\ \lambda_4(z)]^T$ are the *Lagrangian multipliers* (or co-state variables), which are determined by the following co-state equations:

$$\dot{\lambda}(z)=-\left(\frac{\partial\mathbf{f}}{\partial\mathbf{x}}\right)^T\lambda(z)-\left(\frac{\partial L}{\partial\mathbf{x}}\right) \qquad (7)$$

The optimal $K_La(z)$ not considering constraints (4) is solved using:

$$\frac{\partial H}{\partial K_La}=0$$

as:

$$K_La^*(z)=-\frac{k_1+\left(S_O^*-S_O(z)\right)\lambda_2(z)Q/A}{2k_2} \qquad (8)$$

The third and fourth constraints in (4) are satisfied automatically while solving the state equations (5) and can therefore be eliminated. In a wastewater treatment plant, the discharge limit for soluble biodegradable COD is typically achieved when the ammonia nitrogen discharge limit is met. Therefore, the 6th constraint is overwritten by the 5th one. Further, it is apparent that J will be minimised only when the equality of C5 is satisfied. C5 is therefore converted to a boundary condition $S_{NH}(1)=S_{NH,lim}$. The remaining constraints are therefore the control constraint C1, which can be directly imposed to the $K_La^*(z)$ calculated using equation (8), and the state constraint C2. C2 can be considered as follows: the $K_La^*(z)$ calculated using equation (8) should be applied when $S_O(z)>0$; the $K_La^*(z)$ calculated as follows should be used when $S_O(z)=0$:

$$K_La^*(z)=\frac{(1-Y_H)r_h(z)+(1-f_P)(b_AX_A+b_HX_H)}{S_O^*} \qquad (9)$$

Solving equations (5), (7), (8), (when $S_O(z)>0$) and (9)($S_O(z)=0$) simultaneously with consideration of Constraint C1 yield the optimal $K_La(z)$. Eight boundary conditions are required in order to obtain unique solutions, of which $S_{NH}(0)$, $S_{COD}(0)$, $S_O(0)$, $X_S(0)$ and $S_{NH}(l)$ are known. As $S_{COD}(l)$, $S_O(l)$ and $X_S(l)$ are unspecified, the other three boundary conditions are obtained as $\lambda_2(l)=0$, $\lambda_3(l)=0$ and $\lambda_4(l)=0$ (Bryson and Ho, 1975). A two-point boundary-value problem is thus obtained.

3.2 *Optimization Algorithm for Numerical Solution*

Differential equations (5) and (7) can be solved either moving forward (z increases from 0 to l) or backward (z decrease from l to 0). The latter method is chosen in this study since it provides a better numerical stability (data not shown). With the four known 'initial' conditions $S_{NH}(l)$, $\lambda_2(l)$, $\lambda_3(l)$, $\lambda_4(l)$ and four guessed 'initial' conditions $S_{COD}(l)$, $S_O(l)$,$X_S(l)$ and $\lambda_1(l)$, equations(5), (7), (8)and(9) are solved with consideration of constraint C1, yielding the 'end' values of $S_{NH}(0)$, $S_{COD}(0)$, $S_O(0)$ and $X_S(0)$. These values are then compared to their pre-specified values and an optimisation algorithm is initiated to find the $S_{COD}(l)$, $S_O(l)$, $X_S(l)$ and $\lambda_1(l)$ values that enable to produce the pre-specified 'end' values of $S_{NH}(0)$, $S_{COD}(0)$, $S_O(0)$ and $X_S(0)$. A number of iterations are typically required to produce the $S_{NH}(z)$, $S_{COD}(z)$, $S_O(z)$, $X_S(z)$, $\lambda_1(z)$, $\lambda_2(z)$, $\lambda_3(z)$ and $\lambda_4(z)$ trajectories that satisfy all the boundary conditions. The resulting $K_La(z)$ profile is the one that minimises the objection function while satisfying all the constraints. The optimization algorithm is summarised in Figure 1.

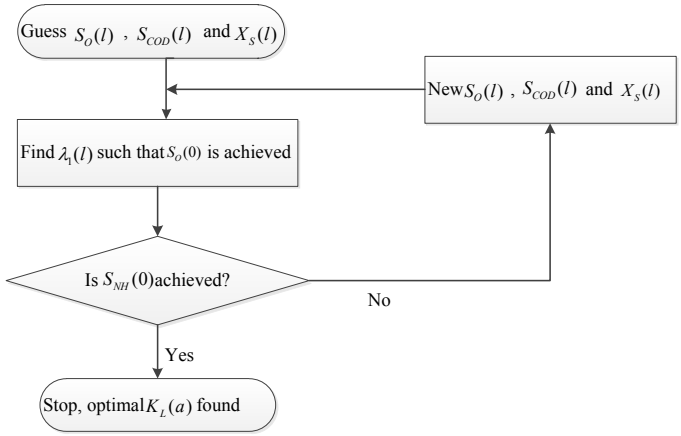

Fig. 1. *The numerical procedure for solving the optimisation problem*

4. RESULTS AND DISCUSSION

4.1 Simulation results

The optimal DO, K_La, ammonium and soluble biodegradable COD profiles obtained in one of the steady-state simulation studies are shown in Figure 2. The effluent ammonium discharge limit of 1gN.m^{-3} is achieved, and the effluent soluble biodegradable COD concentration is almost undetectable. A relatively high K_La is applied at the beginning of the reactor due to the high concentrations of soluble biodegradable COD and ammonia nitrogen in the inlet area. In contrast, aeration is turned off close to the end of the reactor. This makes good sense as further aeration in this part would not further significantly improve nitrification,

while consuming energy. The K_La profile between the two ends of the reactor remains almost constant with a slightly decreasing trend. Correspondingly, DO rises slowly at the beginning of the reactor, and then remains relatively constant with a slightly rising trend, before declining rapidly at the end of the reactor. This sharp DO decrease is beneficial for denitrification in the anoxic reactor (not included in the optimization model) due to reduced oxygen recirculation, although this is not part of the objective function. COD decreases rapidly at the beginning of the reactor, while ammonium decreases almost linearly at a slower rate. It is important to point out that the nitrification rate (data not shown) calculated based on the optimal DO and ammonium concentration profiles is almost constant in sections other than the two ends of the reactor, suggesting that the minimum aeration requirement is achieved through an 'even' distribution of nitrification across the reactor.

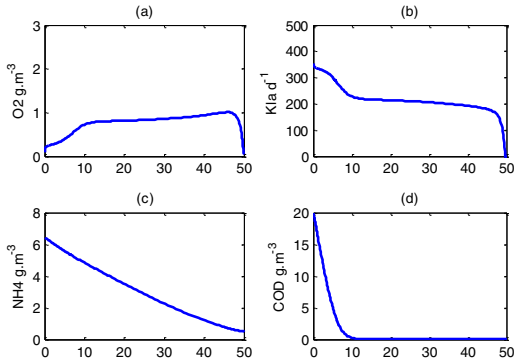

Fig. 2. Results from one steady state simulation study. The effluent ammonium discharge limit was set to 0.5gN.m^{-3}. The maximum and minumum K_La were assumed to be 500 and 0 day^{-1}, respectively. The internal nitrate recirculation flow rate and the return sludge flow rate were assumed to be $Q_{int}=3Q_{in}$ and $Q_r=Q_{in}$, respectively, according to Copp (1999). Therefore, the total flow through the aerobic reactor is $5Q_{in}$. This resulted in an ammonium concentration at the beginning of the aerobic reactor (S_{NH0}) of approximately 6.4gN.m^{-3} (30gN.m^{-3}/5+0.5gN.m^{-3}*4/5) The soluble biodegradable COD concentration at the beginning of the aerobic reactor (S_{COD0}), i.e. the concentration in mixed liqour entering the aerobic reactor, from the anoxic reactor was assumed to be 20g.m^{-3}. Values for all parameters and variables in the model were according to Copp (1999).

Simulation studies were also carried out under numerous other conditions. Figure 3 shows the optimal DO and K_La profiles in two additional sets of simulation studies. In the first set, the ammonium concentration in the feed was increased from 30 to 35, 40 and 45 gN.m^{-3}. As expected, the DO levels (Fig 3A) throughout the reactor increased with increased K_La (Fig 3B), in order to achieve the required level of ammonium removal. However, the patterns observed on both the DO and K_La profiles are very similar to those shown in Figure 2, suggesting the 'optimal' profiles found by the algorithm under different conditions are consistent. In the second set of simulation studies, the internal recirculation rate was varied from 3*Q_{in} (case reported in Figure 2) to 1* Q_{in} and 5*Q_{in}, respectively. The optimal DO and K_La profiles (Fig 3C and 3D) remained very similar to those reported in Fig 2), suggesting that the nitrate recirculation flow rate has a negligible effect of the optimal aeration profiles.

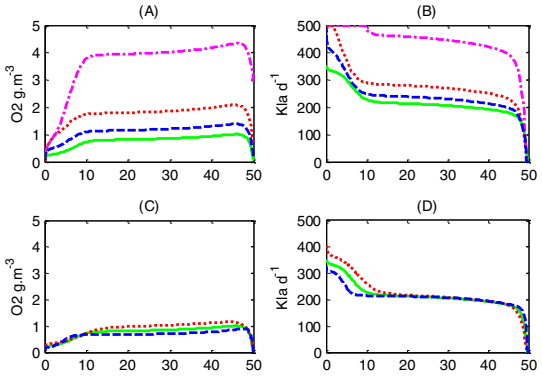

Fig. 3. Optimal DO (A) and K_La (B) profiles with four different influent ammonium concentrations; Solid line: S_{NH0}=30g.m^{-3}; dashed line: S_{NH0}=35g.m^{-3}; dotted line: S_{NH0}=40g.m^{-3}; dash-dot line: S_{NH0}=45 g.m^{-3}. Optimal DO (C) and K_La (D) profiles with three different internal recirculation flow rate; Solid line: Q_{int}= 3Q_{in}; dashed line: Q_{int}=Q_{in}; dotted line: Q_{int}=5Q_{in}.

5. APPLICATION

The optimal DO and K_La profiles can guide how to operate the aerator in practice. In above study cases, the optimal DO and K_La profiles are nearly constant except at the beginning of the reactor. Apparently the effluent ammonia concentration has to be monitored in order to define the required level of the K_La or the DO concentration. A simple consequence of the optimization is to keep the K_La constant in the front reactors and a reduced K_La set-point in the last reactor. Alternatively the DO is kept constant in the front reactors while the DO set-point towards the outlet is governed by the ammonia measurement. This is actually what is used in practice in full scale applications of ammonia based DO control (Åmand et al., 2013).

5.1 *Applied Wastewater treatment Plant Layout*

There are three plant layouts for Matlab simulation. Benchmark case is based on the default open loop IWA benchmark model (Copp, 1999) with the last aerobic reactor's volume divided into a 1200 m3 and a 133 m3 volume respectively. Based on the optimization results the third and fourth aeration zones are supplied with fixed oxygen transfer coefficients (K_La = 10 h^{-1} = 240 d^{-1}) while the fifth and sixth compartments have lower and constant air supply (K_La = 3.5 h^{-1} = 84d^{-1}). Closed loop controllers are provided to keep the K_La constant in the various reactor compartments. The average flow and dry-weather flow are considered for in the steady state and dynamic simulation studies, respectively. In this paper dry-weather data are

considered containing 2 weeks of influent data at 15 min sampling interval. Parameters for the 2 weeks influent are depicted in Figure 4.

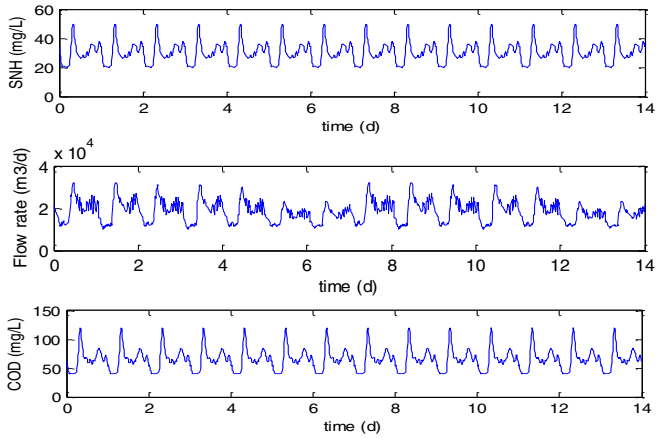

Fig. 4.*Influent Characteristics*

As an alternative result of the optimization the DO is kept constant. Closed loop controllers will provide one DO setpoint in the front aerobic reactors and half the DO set-point for the last reactor.

In order to assess the results between the three cases, a unified effluent criterion is set. The effluent ammonia concentration of the K_La constant case and DO constant case respectively is the same as the benchmark case in both the steady state and dynamic simulation studies.

The aeration energy, AE, defined in the IWA benchmark model (Copp, 1999) is calculated from the K_La in the aerated compartments according to the following formula (valid for Degrémont DP230 porous disks at an immersion depth of 4 m):

$$AE = \frac{24}{T}\int_{t_0}^{t_0+T}\sum_{i=3}^{i=6}\left[0.4032\times K_La(t)_i^2 + 7.8408\times K_La(t)_i\right]dt$$

where K_La is expressed in h^{-1},t_0 is the simulation starting time, T is the period of simulating the plant. For the steady state case t_0=0 days, T=100days and for the dynamic case t_0=7days, T=7days.

The simulation results of steady state flow and dynamic dry weather flow for Benchmark case, KLa constant case and DO constant case are displayed in Table 1.

Table 1. Simulation results assessment

		Openloop Benchmark	K_La Constant	DO constant
Steady state	S_{NH} [g N m^{-3}]	1.67	1.67	1.67
	S_{NO} [g N m^{-3}]	10.45	10.75	10.64
	AE [$kWh.d^{-1}$]	6476	5506	5476
Dynamic	S_{NH} [g N m^{-3}]	4.59	4.59	4.59
	S_{NO} [g N m^{-3}]	8.90	9.12	8.50
	AE [$kWh.d^{-1}$]	6476	5480	5077

For steady state simulation studies, the effluent ammonium and nitrate discharge concentration is achieved to 1.67 g $N.m^{-3}$and around 10.5 g $N.m^{-3}$ among open loop benchmark case, K_La constant case and DO constant case with different energy cost. The highest aeration energy (6476 $kWh.d^{-1}$) is consumed in the Benchmark case, while the K_La-constant case and the DO-constant case use similar amount of aeration energy (5506 $kWh.d^{-1}$ and 5476 $kWh.d^{-1}$ respectively) saving around 15% energy comparing with the Benchmark Case. For dynamic simulation studies, the average effluent ammonium concentration is the same of 4.59 g $N.m^{-3}$ and the average effluent nitrate discharge is 8.90 g $N.m^{-3}$, 9.12 g $N.m^{-3}$ and 8.50 g $N.m^{-3}$ respectively for the open loop benchmark case, K_La constant case and DO constant case. The aeration energy varies between the three cases. The Benchmark case has the highest aeration energy (6476 $kWh.d^{-1}$) while K_La-constant case has aeration energy (5480 $kWh.d^{-1}$) saving around 15.4% of aeration energy and the DO-constant case has an aeration energy (5077 $kWh.d^{-1}$) saving around 21.7% of the energy.

6. CONCLUSIONS

Theoretically optimal DO and K_La profiles in a plug-flow aerobic reactor for aerobic carbon and ammonium oxidation can be computed using the Pontryagin Maximum Principle. The results given for the DO concentration and the K_La should be relatively constant at all locations other than the two ends of the reactor. Aeration should be higher at the beginning of the reactor and be decreasing further downstream and switched off towards the end of the reactor. This provides guidance to aeration control in practical wastewater treatment plants.

REFERENCES

Åmand, L., Olsson, G. and Carlsson, B. (2013). Aeration control - a review. Wat. Sci. Tech. 67(11), 2374-2398.

Alex, J., Beteau, J.-F., Copp, J., Hellinga, C., Jeppsson, U., Marsili-Libelli, S., Pons, M.-N., Spanjers, H., Vanhooren, H. (1999). Benchmark for evaluating control strategies in wastewater treatment plants. In Proceedings of ECC'99, Karlsruhe, Germany.

Bryson, A.E., Ho, Y.C. (1975), Applied Optimal Control, Optimization, Estimation and Control, Hemisphere Publishing Corporation, Washington, DC.

Copp J.B. (1999) Development of standardised influent files for the evaluation of activated sludge control strategies. IAWQ Scientific and Technical Report Task Group: Respirometry in Control of the Activated Sludge Process, IWA Publishing, London.

Copp, J. (2002) The COST Simulation Benchmark: Description and Simulator Manual (J. Copp, ed.), ISBN 92-894-1658-0, Office for Official Publications of the European Community, Luxembourg.

Henze M, Gujer W, Mino T, Van Loosdrecht M. (2000) Activated Sludge Models ASM1, ASM2, ASM2D and ASM3. Scientific and Technical Report No. 9. London: IWA Publishing.

Olsson, G. and Andrews, J.F. (1978). The Dissolved Oxygen Profile - a valuable Tool for the Control of the Activated Sludge Process. Water Research, 12, 985-1004.

Olsson, G. and Andrews, J.F. (1981). Estimation of Loading Changes for the Nitrifying Activated Sludge Process, Paper, IFAC 8th World Congress, Kyoto, Japan.

Olsson, G., Nielsen, M. K., Yuan, Z., Lynggaard-Jensen, A., and Steyer, J-P. (2005) Instrumentation, control and automation in wastewater systems, Scientific and Technical Report No. 11, IWA Publishing, London, UK.

Olsson, G. (2012). ICA and me – a subjective review. Water Res., 46(6), 1585-1624.

Rieger L., Brischke K., Rosso D., Olsson G., Schauer P., Schraa O., Bott C., Johnson B., Shaw A. and Gillot S. (2012) How do we make the best use of dynamic simulators to improve aeration system design? In: 85th Annual Water Environment Federation Technical Exhibition and Conference (WEFTEC 2012), New Orleans, USA.

Rosso, D., Stenstrom, M. K., and Larson, L. E. (2008) Aeration of large-scale municipal wastewater treatment plants: state of the art. Water Science and Technology, 57(7), 973–8.

WEF (2009) Energy Conservation in Wastewater Treatment Facilities - Manual of Practice - No. 32,

Vrečko, D., Hvala, Nadja, and Kocijan, J. (2002) Wastewater treatment benchmark: what can be achieved with simple control? Water Science and Technology, 45(4-5), 127–34.